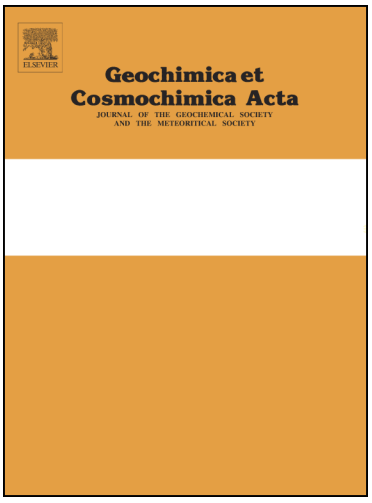

Seawater $^{234}U/^{238}U$ recorded by modern and fossil corals

Peter M. Chutcharavan, Andrea Dutton, Michael J. Ellwood

PII: S0016-7037(17)30793-7
DOI: https://doi.org/10.1016/j.gca.2017.12.017
Reference: GCA 10590

To appear in: *Geochimica et Cosmochimica Acta*

Received Date: 28 May 2017
Accepted Date: 16 December 2017

Please cite this article as: Chutcharavan, P.M., Dutton, A., Ellwood, M.J., Seawater $^{234}U/^{238}U$ recorded by modern and fossil corals, *Geochimica et Cosmochimica Acta* (2017), doi: https://doi.org/10.1016/j.gca.2017.12.017

Seawater $^{234}U/^{238}U$ recorded by modern and fossil corals

Peter M. Chutcharavan[a*], Andrea Dutton[a], Michael J. Ellwood[b]

[1]*Department of Geological Sciences, University of Florida, Gainesville, FL 32611, USA*

[2]*Research School of Earth Sciences, The Australian National University, Canberra, ACT 0200 Australia*

ABSTRACT

U-series dating of corals is a crucial tool for generating absolute chronologies of Late Quaternary sea-level change and calibrating the radiocarbon timescale. Unfortunately, coralline aragonite is susceptible to post-depositional alteration of its primary geochemistry. One screening technique used to identify unaltered corals relies on the back-calculation of initial $^{234}U/^{238}U$ activity ($\delta^{234}U_i$) at the time of coral growth and implicitly assumes that seawater $\delta^{234}U$ has remained constant during the Late Quaternary. Here, we test this assumption using the most comprehensive compilation to date of coral U-series measurements. Unlike previous compilations, this study normalizes U-series measurements to the same decay constants and corrects for offsets in interlaboratory calibrations, thus reducing systematic biases between reported $\delta^{234}U$ values. Using this approach, we reassess (a) the value of modern seawater $\delta^{234}U$, and (b) the evolution of seawater $\delta^{234}U$ over the last deglaciation. Modern coral $\delta^{234}U$ values (145.0 ± 1.5 ‰) agree with previous measurements of seawater and modern corals only once the data have been normalized. Additionally, fossil corals in the surface ocean display $\delta^{234}U_i$ values that are ~5 to 7 ‰ lower during the last glacial maximum regardless of site, taxon, or diagenetic setting. We conclude that physical weathering of U-bearing minerals exposed during ice sheet retreat drives the increase in $\delta^{234}U$ observed in the oceans, a mechanism that is consistent with the interpretation of the seawater Pb-isotope signal over the same timescale.

1. Introduction

The reliability of coral U-series (U-Th) ages can be compromised by subtle post-depositional alteration of the coral skeleton. Several physical and chemical screening procedures, such as X-ray diffraction to determine partial conversion of coralline aragonite to secondary calcite, are frequently used to identify diagenesis in corals. However, these methods do not always identify corals with open-system behavior of U-series isotopes that can bias the calculated date (Scholz and Mangini, 2007). One routine approach to assess whether the U-series geochemistry has been affected is to back-calculate the $^{234}U/^{238}U$ activity ratio, $(^{234}U/^{238}U)_A$, at the time that the coral grew. The $^{234}U/^{238}U$ activity ratio is commonly reported in standard delta notation relative to secular equilibrium:

$$\delta^{234}U\ (‰) = [(^{234}U/^{238}U)_A - 1] * 1000 \quad (1)$$

$\delta^{234}U_i$ represents the initial U-isotope composition of the coral when it grew, and reflects the $\delta^{234}U$ value of ambient seawater ($\delta^{234}U_{sw}$) at the time of coral growth. Due to the relatively long residence time of U in the ocean (~300-500 kyr; Dunk et al., 2002; Henderson and Anderson, 2003), it has previously been assumed that seawater $\delta^{234}U_{sw}$ has remained constant throughout the late Quaternary. Working under this assumption, corals with a $\delta^{234}U_i$ significantly different than the modern seawater value are rejected as altered (Bard et al., 1991; Hamelin et al., 1991; Gallup et al., 1994).

There is debate, however, regarding the appropriate implementation of this screening criterion, both in terms of what value to use for modern $\delta^{234}U_{sw}$ and with respect to the underlying assumption that $\delta^{234}U_{sw}$ has remained constant throughout the late Quaternary (Cheng et al., 2000; Robinson et al., 2004; Esat and Yokoyama, 2006; Andersen et al., 2010; Cheng et

al., 2013; Chen et al., 2016). Box modeling demonstrates that $\delta^{234}U_{sw}$ has probably not changed by more than 10 ‰ over the last 800,000 yrs (Henderson, 2002), but it is not clear what tolerance should be accepted in terms of the departure of back-calculated $\delta^{234}U_i$ coral values from the modern $\delta^{234}U$ composition of the open ocean. There is also some evidence that $\delta^{234}U_{sw}$ may vary on glacial-interglacial timescales based on the observation of lower coral $\delta^{234}U_i$ values during the last glaciation (e.g. Robinson et al., 2004; Esat and Yokoyama, 2006; Esat and Yokoyama, 2010; Chen et al., 2016). However, the relative contribution of diagenetic overprinting in fossil coral geochemistry versus a change in primary seawater signal has not been established, in part, due to lack of an independent means of reconstructing $\delta^{234}U_{sw}$ on these timescales. If $\delta^{234}U_{sw}$ has varied significantly on glacial-interglacial timescales, then excluding corals with $\delta^{234}U_i$ values more than a few permil from modern seawater composition may inappropriately reject unaltered samples. More fundamentally, there are issues in establishing what the accepted value is for modern coral $\delta^{234}U$. When published coral data are updated to the most recent decay constants (Cheng et al., 2013) for ^{230}Th and ^{234}U there appears to be an offset of a few permil between modern seawater (146.8 ± 0.1 ‰, Andersen et al., 2010) and modern coral measurements (145.0 ± 1.5 ‰, Table 1) calling into question: (1) what the accepted modern $\delta^{234}U_{sw}$ value should be, and (2) whether potential offsets in interlaboratory accuracy are confounding the interpretation of the $\delta^{234}U$ measurements for both seawater and corals. Here, we evaluate $\delta^{234}U_i$ in both modern and fossil corals to better characterize modern uranium isotope composition of the surface ocean and to assess the magnitude and timing of variability in $\delta^{234}U_{sw}$.

2. Methods

We compiled 2184 U-series measurements of corals in living in the surface and deep ocean to add to recent compilations (Hibbert et al., 2016; Chen et al., 2016) of coral measurements, yielding a total of 2918 individual U-series measurements for the time frame of 60 thousand years ago (ka) to present (see Supplementary datasets 1 and 2 in Appendix A). Coral U-series measurements for both datasets were normalized to the same decay constants for ^{234}U and ^{230}Th (Cheng et al., 2013, see Section 2.1) and screened for calcite and detrital thorium contamination using a range of different values to define the rejection threshold (Section 2.2). Samples with measured $(^{234}U/^{238}U)_A$ ratios determined by calibration to a secular equilibrium standard (rather than gravimetric) were normalized using reported measurements of the SRM 960 uranium standard (also known as CRM 145 or CRM 112-A; Cheng et al., 2013). This correction was necessary to account for offsets in accuracy introduced by differences between individual aliquots of the secular equilibrium standard Harwell Uraninite (HU-1) and/or between HU-1 and the gravimetrically-determined value of the $^{234}U/^{238}U$ secular equilibrium ratio (Cheng et al., 2013) and is explained in greater detail below. The issues raised and explored here with respect to different approaches to calibrating U-series measurements reinforce the data-reporting guidelines for U-series measurements outlined in (Dutton et al., 2017), including the suggestion that laboratory calibration techniques are explicitly reported in each publication.

2.1 Normalization of reported measurements

Some laboratories employ a secular equilibrium (SE) standard (*i.e.*, $\delta^{234}U = 0$ ‰) such as the Harwell Uraninite (HU-1) to calibrate measurements of $^{230}Th/^{238}U$ and/or $^{234}U/^{238}U$ activity ratios as an alternative to gravimetric spikes. Unlike mixed U-Th spikes or tracers that are

calibrated to U and Th metal standards of known mass, isotope activity ratios calibrated to SE standards do not have to be corrected for recently revised (Cheng et al., 2000; Cheng et al., 2013) ^{234}U and ^{230}Th decay constant values, since the SE standard still has an (assumed) activity ratio of 1. In contrast, measured activity ratios that are calibrated to gravimetric standards need to be corrected to compare data when different sets of decay constant values have been used.

Converting U-series data from laboratories that use SE standards to a different set of decay constants is complicated by two factors. First, laboratories often calibrate the $^{230}Th/^{238}U$ activity ratio to HU-1, yet $(^{234}U/^{238}U)_A$ may be calibrated to a gravimetric standard such as SRM-960. In this case, to update the published activity ratios to a different set of decay constants the $(^{234}U/^{238}U)_A$ ratios still need to be recalculated using the newly-adopted decay constants whereas the $(^{230}Th/^{238}U)_A$ ratio does not need to be revised (because the activity ratio of the SE standard is still 1). We found that $(^{234}U/^{238}U)_A$ ratios that were calibrated using an SE standard required an additional correction given the mismatch between the SE value determined using HU-1 and gravimetric standards (*e.g.*, Cheng et al., 2013) and also due to differences between separate aliquots of HU-1 that are employed in different laboratories. This can be addressed using published $(^{234}U/^{238}U)_A$ values of a gravimetric standard such as SRM 960 to normalize ratios between laboratories. A correction factor can be determined by normalization to an accepted reference value for the standard. In this case, we used the SRM 960 measurement of Cheng et al. (2013) to be consistent with the decay constants also derived in that study. The correction factor (C) can be obtained that corrects for offsets between HU-1, calculated as follows:

$$C = (^{234}U/^{238}U)_{A,\,ref} / (^{234}U/^{238}U)_{A,lab} \quad (2)$$

where the chosen reference activity ratio for SRM 960 (in this case, from Cheng et al., 2013) is divided by the measured activity ratio of SRM 960 from the laboratory where the sample was measured. Uncertainty is propagated using the following equation:

$$\text{Uncertainty} = C * [\ (u_{lab}/x_{lab})^2 + (u_{ref}/x_{ref})^2\ ]^{1/2} \qquad (3)$$

where u_{lab} and x_{lab} are the uncertainty and $(^{234}U/^{238}U)_A$ ratio, respectively, for the reported SRM 960 measurement in that laboratory, and u_{ref} and x_{ref} are the uncertainty and activity ratio for the SRM 960 measurement from Cheng et al. (2013). The normalized value is calculated by taking the measured $(^{234}U/^{238}U)_A$ ratio and multiplying that activity ratio by the correction factor. Due to the decay constants used and the additional $^{234}U/^{238}U$ corrections applied in this study, it should be noted that reported $\delta^{234}U_i$ values in this study may be different from previously published compilations (*e.g.* deep-sea coral $\delta^{234}U_i$ from Chen et al. (2016) versus this study).

Even with the data normalization procedure discussed above, it is still possible that some systematic inter-laboratory offsets are present in the dataset. For example, the $^{238}U/^{235}U$ ratio of a sample is often used to perform a mass bias correction by assuming that this ratio is constant in natural materials (Stirling et al. 2007). This creates a potential systematic bias in that the accepted bulk continental crust $^{238}U/^{235}U$ ratio was revised from 137.88 (Cowan and Adler, 1976; Steiger and Jäger, 1977) to 137.809 ($\delta^{238}U$ = -0.29 ‰, relative to the certified value for CRM-112a) (Tissot and Dauphas, 2015; Noordman et al., 2016; Andersen et al., 2017). In comparison, corals and seawater have $\delta^{238}U$ values ranging from -0.38 to -0.41 ‰ (Stirling et al., 2007; Weyer et al., 2008; Andersen et al., 2014; Tissot and Dauphas 2015). Though $\delta^{238}U$ measurements of groundwater are currently limited to studies concerning ore deposits (e.g. Murphy et al. 2014; Basu et al. 2015; Andersen et al. 2017 and references therein), variability in groundwaters would likely be transferred to speleothems, hence explaining some of the

variability observed in cave samples (-0.7 to +0.44 ‰, Stirling et al., 2007). Using 137.88 for a mass bias correction at the time of measurement would have introduced a small, yet systematic error, and different mass bias corrections may be required when the sample and standard have different $^{238}U/^{235}U$ compositions. Normalization of the value assumed for $^{238}U/^{235}U$ was not undertaken for the data compiled in this study, primarily due to the lack of transparency as to how and when this value is applied in the data reduction process. Fortunately, this error is a sub-permil level correction and therefore should only meaningfully affect high-precision $\delta^{234}U$ measurements, such as the Faraday-Faraday technique employed by Andersen et al., (2010). In the case of the Andersen et al. (2010), this error is important because it provides the most analytically precise (ε-level) measurements of a large suite of seawater samples, however the compiled coral data is characterized by lower precision measurements. Here, we compare three different approaches to correcting the seawater $\delta^{234}U$ value of Andersen et al. (2010). In addition to the normalization to SRM 960, as described above, we also compare this value with that determined in Andersen et al. (2014) for a subset of the same samples, which used a the IRMM 3636 ^{233}U-^{236}U spike to make the mass bias correction, but is reported with lower precision than in the original analysis. Finally, we also correct the reported seawater $\delta^{234}U$ value of Andersen et al. (2010) using the measured $\delta^{234}U$ value for their aliquot of HU-1, which was also determined using the IRMM 3636 mass bias correction.

2.2 Assessing Diagenesis

Fossil corals in this study were subject to two levels of screening based on mineralogical preservation (% calcite) and detrital Th (^{232}Th) content (Fig. A.1). We defined thresholds for

rejecting data for each of these parameters. Samples with measured calcite abundances > 2 % were rejected. This value was chosen because the 2 % level was commonly reported as a lower detection limit in several of the studies (*e.g.*, Yokoyama et al., 2001; Edwards et al., 2003; Scholz and Mangini, 2007). While some modeling suggests that as much as 0.2 % calcite can impact the C-14 age of fossil corals (Chiu et al., 2005), because of the differences in the chemistry of C versus U and T isotopes during diagenesis, it is not clear that the same tolerance applies to U-series ages. Ideally, only coral samples with no detectable calcite should be selected for analysis. However, this proved difficult in practice for the data compiled here, as the definition for "no detectable calcite" varied between different studies (e.g. different calcite detection limits, no mention of detection limit, etc.). Although U-series measurements can be corrected for detrital Th content, this requires knowledge of the contaminant $^{230}Th/^{232}Th$ activity ratio, which is likely to be site-specific. Some studies involving Last Interglacial corals have used a threshold of 2 ppb ^{232}Th for detrital Th screening (*e.g.*, Scholz and Mangini, 2007), but this same level of detrital Th has a greater effect on younger coral ages. Given the wide range of coral ages in considered in this study, we adopted a different approach, using a sliding scale for screening according to ^{232}Th concentration. Samples were binned by age and screened by ^{232}Th content, using an increasing tolerance of ^{232}Th concentration with age, to account for the fact that a given ^{232}Th concentration will have less effect on detrital Th age corrections with increasing sample age. Samples with ages younger than 5,000 years were rejected if ^{232}Th content exceeded 0.1 ppb in accordance with the recommendations of Cobb et al. (2003). In the Cobb et al. (2003) study, this level of contamination has less of an effect on corals older than 5,000 years ago (ka), so from 5-20 ka the threshold was increased to 1 ppb while corals from 20-60 ka were screened using a 2 ppb threshold.

Here we define two separate screening scenarios based on detrital Th content and % calcite. In the first scenario, which we refer to as "screened", samples without % calcite or ^{232}Th data reported or that stated that the parameter was "below detection limits" were assumed to pass the defined screening criteria as well as any samples that were below the screening thresholds defined above. In the second scenario, which we refer to as "strictly screened", data with no reported values for the screening parameters were also excluded. However, most of the data for recent and deep-sea corals compiled in this study did not report calcite abundance, so we did not apply this second scenario to the modern or deep-sea corals. Additionally, most deep-sea corals (including modern) had elevated ^{232}Th concentrations, so we instead used a uniform threshold value of >2 ppb [^{232}Th]. The data were also examined to determine if differences in $\delta^{234}U_i$ could be explained by other factors such as post-depositional exposure history (*i.e.*, whether the corals are currently exposed above sea level or submerged), ocean basin, locality, and/or coral taxa.

2.3 Statistical analysis of shallow-water coral $\delta^{234}U_i$ data

Statistical assessment of the shallow-water coral data was performed on the "screened" dataset, as defined above. The average modern coral δ^{234}U value was determined by taking the inverse-variance weighted mean (IVWM) of the screened coral data compiled for the past 300 years. All reported means in the main text are weighted means with 2σ uncertainties. The median and standard deviation from the mean were also calculated for each time slice (time slices defined in Section 3.2).

Statistical significance of whether the mean value of fossil coral $\delta^{234}U_i$ changed through time was determined using two-sided t-tests and a simple bootstrap randomization test with replacement. As the data in our compilation is not normally distributed, the bootstrap is useful as

a second, non-parametric check on the t-test results. In this study, the difference between the mean $\delta^{234}U_i$ value for a time slice and the modern value was considered statistically significant if there was a greater than 95% probability ($p < 0.05$) that the mean has a $\delta^{234}U_i$ value different than that of modern coral $\delta^{234}U_i$. Means and statistical analyses were made using the programming language R.

2.4 Evaluating riverine $\delta^{234}U$ on glacial-interglacial timescales

In their study of deep-sea coral $\delta^{234}U_i$, Chen et al. (2016) used a compilation of speleothem U-series measurements to argue that magnitude of variations in continental weathering rates from the mid-low latitudes is not large enough to cause the changes in $\delta^{234}U_{sw}$ inferred from the coral record. Here, we do not argue that speleothems are a reasonable representation of riverine input, but we briefly revisit the speleothem archive to clarify the observational records and how this contributes to the continental weathering signal. Variability in speleothem $\delta^{234}U_i$ from the compilation shown in Chen et al. (2016) was re-evaluated by performing a two-sample t-test to determine if the mean $\delta^{234}U_i$ value for Holocene U-series data was statistically significantly different ($p < 0.05$) from the mean $\delta^{234}U_i$ value for samples that were glacial to Holocene in age within the same speleothem. We calculated the percent change from the mean of each $\delta^{234}U_i$ value for specimens that displayed variability, i.e., for those speleothems where pre-Holocene $\delta^{234}U_i$ values were statistically significantly different than Holocene compositions. This allows us to easily compare how the $\delta^{234}U_i$ values are varying between each speleothem record (i.e. the mean $\delta^{234}U_i$ value for the speleothem always = 0 %). We also compiled data for additional several speleothems that span multiple glacial-interglacial

cycles to see if the $\delta^{234}U_i$ values vary with these cycles. To assess the composition of riverine $\delta^{234}U$ over time, we used a simple box model to explore the parameter space that would satisfy the observations in terms of variability in seawater $\delta^{234}U$ through time. This approach is similar to previous box modeling (Henderson, 2002; Robinson et al., 2004; Chen et al., 2016). The parameterization and set up of the model is provided in the supplementary text (Table A.1, Fig. A.2). Our objective was to use this tool to quantify the required flux and composition of riverine input to explain the observed signal in the oceans.

3. Results

3.1 Modern $\delta^{234}U_{sw}$

The modern coral data have a mean value of 145.0 ± 1.5 ‰ (n=137), with a median and standard deviation of 145.1 ‰ and 1.8 ‰, respectively (Table 1). In this study, we defined "modern corals" as those that are younger than 0.3 ka. Adjusting the age cutoff for the definition of modern to a value between 0.1 and 1 ka does not change the mean value by more than 0.1 ‰. The importance of our 2-step procedure to normalize $\delta^{234}U$ measurements (1) by normalizing to the same decay constants (Table 2), and (2) correcting for the calibration techniques employed in the original studies, becomes apparent when comparing reported measurements of modern corals and seawater (Fig. 1, Table 3). The $\delta^{234}U_i$ value of modern corals compiled for this study (145.0 ± 1.5 ‰) is nearly 2 ‰ lower than the typically accepted value of modern, open ocean seawater (146.8 ± 0.1 ‰) that was determined using an analytical approach with epsilon-level precision and calibrated to an HU-1 standard (Andersen et al., 2010). However, when the activity ratio for the modern seawater measurements by Andersen et al. (2010) is corrected by reference to the measured value for the SRM 960 standard in that laboratory (Section *2.1*), the $\delta^{234}U_{sw}$ value of

the seawater measurements drops to 144.9 ± 0.4 ‰., in agreement with our compiled coral data. We also tested two other means of correcting the Andersen et al. (2010) $\delta^{234}U_{sw}$ value, as explained in the methods but not shown on Figure 1. These include adjusting the value based on a new (more accurate but less precise) measurement of some of the same seawater samples (145.7 ± 0.5 ‰; Andersen et al., 2014) and also by using the gravimetrically-determined value for their HU-1 aliquot (-0.9 ± 0.4 ‰; Andersen et al., 2015), which would bring the $\delta^{234}U_{sw}$ value to 145.8 ± 0.6 ‰. All three of these approaches to correcting the $\delta^{234}U_{sw}$ value of Andersen et al. (2010) slightly lower the value originally reported in Andersen et al. (2010) and bring it within uncertainty of the modern coral value determined from our data compilation.

3.2 Coral $\delta^{234}U_i$ from LGM-present

Having established the modern U-isotope composition of seawater and corals, we turn to the fossil coral record to assess the evolution of seawater $\delta^{234}U$. For fossil shallow-water corals, we somewhat arbitrarily divided the record into four time-intervals to characterize the $\delta^{234}U_i$ variability (e.g. Fig. 2d, Table 1). The first interval (29 to 21 thousand years ago (ka)) records a value of 137.8 ± 1.1 ‰ (n=41), ~7 ‰ lower than the modern value. We note that only during this time interval, there may be a difference in the $\delta^{234}U_i$ value recorded in different ocean basins in the surface ocean, where the mean Pacific data may be ~ 2 ‰ higher (139.8 ± 1.4 ‰) than the mean Atlantic (137.1 ± 1.0 ‰) (Fig. 3, Table 4). This conclusion is tentative because of the decreased density of data in this time interval. The LGM $\delta^{234}U_i$ mean of all the data is ~7 ‰ lower than modern, thus we conservatively interpret this value as ranging between 5 and 7 ‰ lower because of this possible inter-basin difference. No inter-basin differences are observed in the remainder of the compiled shallow-water coral record. After the LGM, there is a transition

period from 21 to 17 ka marked by an abrupt increase in $\delta^{234}U_i$ to 140.7 ± 1.1 ‰ (n=59) over a few thousand years and in-step with the onset of deglaciation (Clark et al., 2009). A gap in the shallow-water coral data occurs between ~17.5 and 16 ka, coincident with the timing of Heinrich Event 1 (H1) in the North Atlantic (Hemming, 2004, Fig. 3). By the time the record reestablishes itself around 16 ka, $\delta^{234}U_i$ values are much closer to the modern coral value of 145.0 ± 1.5 ‰, recording a value of 143.7 ± 0.8 ‰ (n=300) for the time interval from 17 ka to the Pleistocene-Holocene boundary (11.7 ka, Walker et al., 2009). Both the t-test and bootstrap analysis (Section 2.3) indicate that the lower mean LGM and early deglacial $\delta^{234}U_i$ values are statistically different ($p < 0.05$) than the modern value of shallow water corals (Table 1, A.2, A.3).

From 11.7 ka to present, there is a difference between coral $\delta^{234}U_i$ values (144.8 ± 0.9 ‰, n=436) and the modern value, but the magnitude of this difference is small (~0.2 ‰). We do not quantify potential shorter-term variability in $\delta^{234}U_{sw}$ using the compiled data set because ephemeral shifts require high-temporal density datasets developed within a single laboratory due to the lingering potential for interlaboratory offsets that may not have been captured in our data normalization procedure.

Results for screened, shallow-water corals (Table 1) demonstrate that modern corals have the least variability (one standard deviation [s.d.] = 1.8 ‰, while deglacial corals (17-11.7 ka) have the most variability (1 s.d. = 4.6 ‰). Corals from early in the deglacial (17-21 ka) and during the LGM had somewhat more variability than modern corals (1 s.d. = 2.3 ‰ for both time slices).

3.3 Pre LGM coral $\delta^{234}U_i$

The pre-LGM, Marine Isotope Stage (MIS) 3, data is sparse in comparison to the deglacial record and appears to contain more scatter. Based on the available data, the $\delta^{234}U_i$ value of MIS 3 corals is consistently lower than modern seawater but most of the data are somewhat higher than the LGM minimum prior to 30 ka (Fig. 2). Given the sparseness and high variability within the data for this time-period, we do not make any firm assessments of trends or compositions. Most of the data in this time window come from Papua New Guinea and Vanuatu, where uplifted sequences of coral terraces are exposed.

3.4 Deep-sea corals

Changes in deep-sea coral $\delta^{234}U_i$ over the past 60 ka are shown in Figure 4. Deep-sea corals appear to record an abrupt increase in $\delta^{234}U_i$ of ~10 ‰ at ~16.5 ka, several thousand years after the increase in $\delta^{234}U_i$ in shallow-water corals is initiated at the end of the LGM. This shift may be real, but at this stage we cannot rule out the possibility that the apparent shift may be an artifact of a lack of data from the sites higher than 30°N in the N. Atlantic in the time window just prior to the onset of the deglaciation. Additionally, the different ocean basins show some differences in the absolute values and temporal trends in $\delta^{234}U_i$ for the deep-sea corals; high-latitude (i.e. >30 °N) N. Atlantic deep-sea corals at 17 ka have higher $\delta^{234}U_i$ values compared to other regions except for the Southern Ocean (Fig. 4). The timing of the shift at 17 ka is broadly coincident with the timing of the H1 event in the N. Atlantic. The Southern Ocean $\delta^{234}U_i$ deep sea record is somewhat more continuous from 40 ka to present, showing a gradual increase in coral $\delta^{234}U_i$ until ~16 ka, after which both the data density and the $\delta^{234}U_i$ values increase. As reported in Chen et al. (2016), low-latitude North Atlantic corals display an increase of a 3-4 ‰

from the LGM to the Holocene, with an ephemeral increase during HS1 that overshoots the Holocene values by a few permil. Trends within the other ocean basins are more difficult to discern owing to high scatter and variable data density over time.

3.5 Speleothem $\delta^{234}U_i$

We assessed changes in $\delta^{234}U_i$ that are recorded in speleothems that span the LGM to present to evaluate whether groundwater compositions in carbonate catchments were changing due to weathering on glacial-interglacial cycles. The difference in means of Holocene vs pre-Holocene speleothem $\delta^{234}U_i$ was significant for 12 of the 18 compiled records and 10 of these speleothems show a decrease in $\delta^{234}U_i$ during the last deglaciation (Fig. 5). One speleothem (C996-2) did not have enough data points during the deglacial period to ascertain a trend and only one speleothem not shown in Figure 5 (SSC01) showed an increase in $\delta^{234}U_i$ during the deglacial. This indicates that in places where the chemical weathering on glacial-interglacial timescales induces a change in $\delta^{234}U$ of the speleothem (as a proxy for groundwater), the sense of that change is inverse to that observed in the corals (as a proxy for seawater). Also, our observations contradict the assertion of Chen et al. (2016) that speleothem records do not show any meaningful change in $\delta^{234}U_i$ during the last deglaciation. Similar changes are observed in longer speleothem records covering multiple glacial cycles, where the $\delta^{234}U_i$ value decreases during the interglacial periods (Fig. A.3).

We performed a suite of box-modeling experiments to see if we could replicate the shift observed in seawater uranium isotope composition. Our modeling is consistent with the results of previous studies (Henderson, 2002; Robinson et al., 2004; Chen et al., 2016). The box model

experiments were able to replicate the change in $\delta^{234}U_{sw}$ observed in the shallow-water coral record using pulsed inputs for changes in riverine input at the start of the deglacial (Fig. 6a,b). We found that increasing the duration of the pulse decreased the pulse amplitude required to cause a ~7 ‰ change between the LGM and the present. The 2, 5 and 10 kyr pulses required pulse amplitudes of approximately 2500 ‰, 1100 ‰, and 700 ‰, respectively for $\delta^{234}U_{input}$ (Fig. 6c). In scenarios where ^{238}U input was varied, the pulses for 2, 5 and 10 kyr required amplitudes of approximately 19, 8, and 4 times greater, respectively, then the starting ^{238}U input rate (Fig. 6d). Hence, increasing the amount of ^{238}U delivered to the oceans, increasing the $\delta^{234}U$ value of the input, or some combination of the two can create the observed shift in seawater composition.

4. Discussion

Our data compilation reveals interesting offsets between modern coral and seawater values measured in different studies as well as between laboratories. We also documented a robust, rising trend in coral $\delta^{234}U_i$ between the LGM and present. Here we further evaluate the significance of these observations.

4.1 Modern coral and seawater $\delta^{234}U$

The weighted-mean value of screened modern corals was found to be 145.0 ± 1.5 ‰ using the two-step normalization process that both normalizes all of the data to the same ^{234}U decay constant and normalizes between different calibration methods. As explained in Section 2.1, the corrected $\delta^{234}U_{sw}$ value of Andersen et al. (2010) shown in Figure 1b is different from the value originally reported, and is interpreted as arising from the difference between the

$(^{234}U/^{238}U)_A$ ratio of the HU-1 (SE) standard used in the study and the SE value predicted using the ^{234}U decay constant in Cheng et al. (2013) and the ^{238}U decay constant of Jaffey (1971). This observation combined with the range of reported values for SRM 960 in different laboratories employing the HU-1 standard implies that (a) the $^{234}U/^{238}U$ composition of HU-1 is not the same as the gravimetrically determined value of Cheng et al. (2013), and (b) that different aliquots of HU-1 can have different $(^{234}U/^{238}U)_A$ ratios that are resolvable, particularly when using epsilon-level precision measurement techniques (e.g. Andersen et al., 2004).

4.2 Evaluating the robustness of the temporal trend in coral $\delta^{234}U_i$

To assess whether the apparent positive shift in coral $\delta^{234}U_i$ from the LGM to present is a reflection of seawater $\delta^{234}U$ rather than an artifact of other confounding factors we compared different subsets of the data. First, we consider the potential for contamination of the coral $\delta^{234}U_i$ signal by initial detrital Th (and associated U) or by diagenetic overprinting caused by open-system behavior. Even after screening out potentially altered samples, the fundamental observation that coral $\delta^{234}U_i$ has increased since the LGM remains, regardless of the diagenetic screening criteria applied (Fig. A.1). In other words, screening out altered samples does not remove the trend from the LGM to present, and if anything, accentuates it. There is still scatter in $\delta^{234}U_i$ values within any given time slice even after screening the data, some of which may be due to diagenesis that is not detected by the screening technique. However, we note that even the modern corals display scatter (95 % of the data lie within 4 ‰ of the mean) that is larger than what would be expected based on the reported analytical uncertainties alone. It is not clear whether this observation in modern corals is the result of: (1) local departures to the open ocean

seawater composition in fringing reef environments where surface runoff (with higher $\delta^{234}U$) mixes with seawater, (2) possible unaccounted offsets in interlaboratory accuracy, or (3) early marine diagenesis.

Thus, to further assess the pattern of coral $\delta^{234}U_i$ rise observed between the LGM and present, we compared the trend between subsets of the data with different diagenetic histories (subaerial exposure versus marine submergence), different coral taxa, different ocean basins, and between surface ocean and deep-sea corals to determine if any of these factors can explain the apparent difference in $\delta^{234}U$ between LGM corals and modern seawater. Each subset of the data displays a rise in $\delta^{234}U_i$ between the LGM and present, although for the deep-sea corals, the magnitude of the change in $\delta^{234}U_i$ may be different than that observed in the surface ocean corals and varies by geographic location (Fig. 4, also see Chen et al., 2016). Both exposed and submerged surface ocean corals display a positive shift in $\delta^{234}U_i$ after 21 ka, indicating that this shift occurs, regardless of the post-depositional diagenetic environment (Fig. 7a). The positive shift from LGM to present is also visible in within different coral taxa through time indicating that the change is not a function of different taxa between the different time periods (Fig. 7b). Surface ocean corals from the Indo-Pacific and Caribbean both show an increase in $\delta^{234}U_i$ values from the LGM to present (Fig. 3). This same trend is present within multiple individual localities (*e.g.*, Great Barrier Reef, Barbados, French Polynesia, Papua New Guinea, and Vanuatu, Fig. 8). These observations combined with the result that diagenetic screening also does not change the overall pattern, indicates that the pattern of rising coral $\delta^{234}U_i$ from the LGM to present is a primary signal of seawater composition changing through time.

Prior to the LGM (30-60 ka) there is substantial scatter and sparseness of data. However, the shallow-water coral $\delta^{234}U_i$ values from 30-50 ka do appear to be generally higher (~140 ‰)

than during the LGM, but still lower than modern seawater. Unfortunately, there is virtually no Caribbean coral data prior to 30 ka, which precludes a direct comparison between ocean basins during this time window. To evaluate seawater $\delta^{234}U$ values during this time window more rigorously requires increased data density and would also benefit from data collection at sites other than Huon Peninsula and Vanuatu, which dominate the dataset in this time window.

4.3 Diagenesis in Shallow-Water Corals

One critique of using shallow water corals to reconstruct changes in seawater chemistry over time is that they are susceptible to open-system diagenesis. Despite our demonstration that the upwards shift in $\delta^{234}U_i$ from the LGM to present, regardless of diagenetic history, location, or taxa, it is clear that applying various levels of screening to the data does not completely remove samples which may contain diagenetic overprinting from the compilation. Because it is not always clear where the subtle effects of diagenesis may affect the record, we hesitate to over-interpret the record in terms of short-term changes or the offsets observed in the data compilation. We note that even after screening is applied, there are still six coral measurements with $\delta^{234}U_i$ values that lie above and 36 measurements that lie below the plotted range for shallow-water corals in Figure 2a. For deep-sea corals, 18 $\delta^{234}U_i$ values lie above and eight lie below the plotted range in Figure 4a (note the slight difference in y-axis scale between this panel and Fig. 2a). Potential diagenetic mechanisms for anomalously high/low $\delta^{234}U_i$ values in corals have been examined extensively in the literature. Diagenetic alteration resulting in anomalously high $\delta^{234}U_i$ values is commonly attributed to weathering processes that preferentially leach crystal lattice sites damaged by alpha-recoil (e.g., Gallup et al. 1994; Fruijtier et al., 2000;

Thompson et al., 2003; Scholz et al., 2007). U-remobilization has also been cited as a potential cause of elevated $\delta^{234}U_i$ values in fossil deep-sea corals (e.g. Cheng et al., 2000; Robinson et al., 2006). Importantly, diagenesis typically elevates the $\delta^{234}U_i$ value, whereas the older (LGM and MIS 3) corals display lower $\delta^{234}U_i$ than modern, which is the opposite of what would typically be expected during diagenesis. The compilation also demonstrates that anomalously low $\delta^{234}U_i$ values can still occur, which is an indication that there are multiple diagenetic pathways that can affect U and Th isotopes when these fossil corals behave as open systems as pointed out in previous studies (e.g., Stirling and Andersen, 2009). Because of the pervasiveness of diagenesis in the pre-MIS 3 fossil coral record (e.g., Hibbert et al., 2016) it remains important to develop a better understanding of open-system diagenesis of the U-series isotope system and explore novel approaches to separate out samples that are diagenetically altered versus those that retain a primary seawater signal.

4.4 Deglacial Deep Sea Coral $\delta^{234}U_i$

Chen et al. (2016) used $\delta^{234}U_i$ measurements from low-latitude Atlantic and Pacific deep-sea corals and a compilation of published deep-sea coral $\delta^{234}U_i$ measurements as evidence for a 3-4 ‰ difference between the LGM and Holocene and a transient spike of approximately 6 ‰ during deglaciation. Unlike the surface-ocean coral data we compiled that show the same value and temporal trends in $\delta^{234}U_i$ regardless of ocean basin, there are differences observed in the deep-sea coral $\delta^{234}U_i$ data between different ocean basins. This indicates that the overall deep-sea coral dataset shown in Figure 4a is subject to biases based on geographic location. Additionally, the deep-sea coral dataset as a whole displays more scatter in the data, particularly within some

geographic regions. This may be a primary signal, or it may be a consequence of the imprint of contamination from oxide crusts. For example, the North Atlantic and Southern Ocean data display more scatter and higher values, particularly during the latter half of the deglacial transition (Fig. 4). It is not clear if this is a primary (seawater) signal or if it is the result of the influence of contaminants. Since the introduction of elevated $\delta^{234}U$ input into the ocean during the deglaciation is thought to be derived from high-latitude weathering (see ensuing section), the abrupt increases, high values, and high scatter observed in the N. Atlantic and Southern Ocean deep sea corals may be recording deglaciation of the proximal high-latitude ice sheets.

One key advantage for the approach of Chen et al. (2016) is that the fossil deep-sea corals were all measured with in the same laboratory using a single experimental protocol. This avoids many of the potential pitfalls inherent to the literature compilation presented here (e.g. systematic inter-laboratory biases, inconsistent diagenetic screening between different labs, different assumptions about $^{235}U/^{238}U$ activity ratios, etc.). Internally-consistent U-series measurements are needed to resolve ongoing questions about $\delta^{234}U_{sw}$, such as potential offsets between ocean basins, which have been discussed here. Fortunately, the change in shallow-water coral $\delta^{234}U_i$ is captured by an internally-consistent study from Barbados (Fairbanks et al., 2005), and by the IODP 310 U-series measurements from Tahiti, which were measured by two laboratories with several duplicate measurements for inter-lab comparison (Thomas et al., 2009; Deschamps et al., 2012). Thus, our data compilation includes records of increasing deglacial surface coral $\delta^{234}U_i$ values from both the Pacific and Atlantic ocean basins, which is corroborated by increasing $\delta^{234}U_i$ observed an internally-consistent dataset of low latitude deep-sea corals (Chen et al., 2016).

4.5 Mechanisms for deglacial change in seawater $\delta^{234}U_i$

Two potential mechanisms have previously been proposed to explain temporal variability in $\delta^{234}U_{sw}$. The first of these (Robinson et al., 2004; Andersen et al., 2013; Chen et al., 2016) invokes enhanced physical weathering due to the retreat of ice sheets during the last deglacial that contributes excess ^{234}U to the oceans. Another hypothesis is that such a shift in $\delta^{234}U_{sw}$ could be accomplished by releasing ^{234}U trapped in reduced sediments from continental margins sediments in-step with deglacial sea-level rise (Esat and Yokoyama, 2006). We also re-examined speleothem $\delta^{234}U$ data to assess the potential riverine input from carbonate catchments. Weathering of limestone catchments and, to some extent, U-rich black shales is considered to be the dominant source of U to the ocean (Palmer and Edmond, 1993). We note that carbonate catchments are only estimated to account for ~8-13 % of continental surface lithology (Amiotte Suchet et al., 2003; Dürr et al., 2005; Hartmann and Moosdorf, 2012). Additionally, U-mobility within groundwater is affected by a number of processes such as redox conditions (e.g. Chabaux et al., 2003; Charette et al., 2008) and local heterogeneity in cave plumbing systems (Zhou et al., 2005). For these reasons we do not expect that speleothem $\delta^{234}U$ variability to be representative of global riverine input as a whole; yet it is interesting to note that the sense of variability in the speleothems that do show glacial-interglacial changes are out of phase with the observed variability in seawater $\delta^{234}U$ (Fig. 5). Hence other contributions must effectively "swamp out" this signal to drive the changes that are observed. Through our box modeling experiments, we found that an abrupt pulse in either total U or $\delta^{234}U$ values was required to simulate the sharp observed transition during the deglacial in the coral data.

A recent study of deep-sea coral $\delta^{234}U_i$ implicates subglacial physical weathering as the driving mechanism for seawater $\delta^{234}U$ variability between the LGM and present (Chen et al., 2016). Discrepancies in $\delta^{234}U_i$ in deep-sea corals from different ocean basins indicates that $\delta^{234}U$ values may be distinct between deep water masses—an observation that merits further study—whereas $\delta^{234}U_i$ in our tropical surface ocean compilation does not show inter-basin differences during the deglaciation. Notably, our compilation of shallow-water corals indicates that a large increase in $\delta^{234}U_{sw}$ occurred earlier in the deglaciation than indicated by the low-latitude deep-sea corals in Chen et al. (2016) (e.g. Fig. 2, 4a). Based on the weighted means for the LGM and early deglacial (137.8 ‰ and 140.7 ‰, respectively; Table 1), approximately 40 % of the increase in $\delta^{234}U_i$ for surface corals occurred between 21-17 ka (an ~3 ‰ shift), coincident with the initiation of ice sheet retreat (Clark et al., 2009). This change is observed in both the Pacific and Atlantic-ocean basins. The tropical deep-sea coral record of Chen et al. (2016) is poorly resolved over this transition, making a direct comparison difficult.

We note that the highest $\delta^{234}U_i$ values for deep-sea corals are recorded in the high-latitude North Atlantic and the Southern Ocean, which is consistent with the idea that the high latitudes are the source of the material driving the deglacial shift in seawater composition. Additionally, most of the increase in $\delta^{234}U_i$ for both the shallow-water and deep-sea coral records appears to occur early in the deglaciation, when sea level had not yet risen much above the LGM lowstand. If the increase in $\delta^{234}U_{sw}$ was tied entirely to sea level (e.g. the U-shelf hypothesis of Esat and Yokoyama 2006), then one would expect the coral $\delta^{234}U_i$ record to increase gradually in-step with sea-level rise. Thus, we conclude that the deglacial increase in $\delta^{234}U_i$ observed in both the surface and deep ocean may have been driven by exposure of freshly-weathered bedrock and

sediment during deglaciation (Foster and Vance, 2006), by contributions from sub-glacial melting (Chen et al., 2016), or both.

Additional support for a link between enhanced high-latitude weathering and deglacial $\delta^{234}U_{sw}$ variability is provided by Pb-isotope records from ferromanganese deposits in the North Atlantic (Foster and Vance, 2006; Crocket et al., 2012). Lead isotopes, which are the end-products of U decay chains, also become more radiogenic in North Atlantic during the deglaciation between 21 and 8 ka (Fig. 2c). Two additional studies of North Atlantic ferromanganese oxides (Gutjahr et al., 2009; Kurzweil et al., 2010) display the same deglacial trend in Pb-isotopes yet also show a decrease in the amplitude of the radiogenic Pb signal with decreasing latitude. This was interpreted by Crocket et al. (2012) as evidence that the Pb-isotopes record a regional continental weathering signature from the Laurentide ice sheet during the last deglaciation. In contrast, recent Pb-isotope measurements from Southern Ocean deep-sea corals do not record any significant glacial-interglacial difference in radiogenic isotope composition (Wilson et al., 2017). This may indicate that weathering of glaciated terranes is not a major driver of Pb-isotope variability in the Southern Ocean or, perhaps, that physical weathering rates were not as high as glaciated regions in the Northern Hemisphere following the LGM. Another possibility is that the deep-sea corals were located too far from the Antarctic margin to record a deglacial shift in Pb-isotopes, as Pb is highly particle reactive and tends to be deposited close to its weathering source. Indeed, the deep-sea corals from Wilson et al. (2017) were located ~2500 km from the Antarctic margin, while the ferromanganese samples from Orphan Knoll (Crocket et al., 2012) were situated a mere 500 km from the Newfoundland coast. In constrast, Pb-isotope records from Blake Ridge, ~3000 km south of Orphan Knoll (Gutjahr et al., 2009) do not show a radiogenic shift in Pb-isotopes during the deglaciation, which is consistent with the hypothesis

that the deglacial increase in North Atlantic Pb-isotopes is being driven by weathering from the high latitudes.

It is also useful to look at other evidence to infer how continental weathering and, by extension, U-isotope transport to the ocean may have varied between glacials and interglacials. U-series measurements from regolith profiles have been used extensively to study continental weathering rates (e.g. Chabaux et al., 2011; DePaolo et al., 2012; Dosseto and Schaller, 2016). There is both experimental (Andersen et al., 2009) and field evidence that leachable U is quickly depleted in freshly-weathered regolith, often within the span of a few hundred years (Ma et al., 2010; Andersen et al., 2013). Thus, periods of rapid exposure of freshly-weathered sediment at the onset of deglaciations (e.g. Reyes et al., 2014) are a potential source of excess ^{234}U to the ocean. This is supported by measurements of riverine $\delta^{234}U_i$ values, which have routinely shown that high-latitude rivers draining deglaciated terranes have $\delta^{234}U_i$ values that are several-hundred per mil higher than mid-low latitude rivers (e.g. Dunk et al., 2002; Henderson and Anderson, 2003; Andersen et al., 2013), while some surface waters in New Zealand and the McMurdo dry valleys in Antarctica are an order of magnitude higher (Robinson et al., 2004; Henderson et al., 2006). Taken together, these studies suggest that enhanced physical weathering of U- and Pb-bearing minerals from the Northern Hemisphere may be an important driver of $\delta^{234}U_{sw}$ and Pb-isotope variability during the deglaciation. Our box modeling experiments indicate that increasing the total flux (amount of ^{238}U) delivered to the oceans, increasing the $\delta^{234}U$ value of the input, or some combination of the two can create the observed shift in seawater composition. It is likely that both processes were at work during the deglacial transition and contributed to the shift in seawater composition.

4.6 Implications for $\delta^{234}U_i$ screening of fossil corals

Given the identification of a ~7 ‰ upwards shift in seawater $\delta^{234}U$ between the LGM and present, it is worth revisiting recommended procedures for screening (culling) U-series measurements on the basis of anomalous $\delta^{234}U_i$ values; as has been standard practice in the past. Initially, studies screened around a modern seawater value, working under the assumption that seawater $\delta^{234}U$ does not changed significantly on glacial-interglacial timescales. For the IntCal13 radiocarbon calibration curve, however, the difference between fossil coral $\delta^{234}U_i$ values from the Holocene and the last glacial period was addressed using a two-step screening procedure (Reimer et al., 2013). For fossil corals with ages <17 ka, a tolerance of 147 ± 7 ‰ (3σ) was used based on a compilation of young and modern fossil corals, while glacial-age corals with ages >17 ka were screened using a tolerance of 142 ± 8 ‰ (3σ). When these two values are shifted to reflect the revised $\delta^{234}U_i$ value for modern corals presented in this study, the new screening thresholds would become 145 ‰ for <17 ka and 140 ‰ for 17 ka – 60 ka. These criteria are consistent with our interpretations of changes in seawater composition across the time window captured by radiocarbon dating. Even though it is possible to achieve high-precision U-series measurements of corals and seawater samples, we would still recommend using a fairly generous tolerance for uncertainty around the chosen screening value given that 95% of the screened modern data fall within 5 ‰ of the modern seawater $\delta^{234}U$ value (145 ‰). We note again, that the variance observed in modern corals is greater than anticipated solely based on the reported analytical uncertainty. This may indicate a superposition of additional inter-laboratory biases or natural variability in modern reef systems, which should be investigated in addition to traditional open-water seawater measurements.

Using the data we have compiled, it would be possible to further refine the screening criteria across the deglacial transition according to the weighted means reported in the second and third columns of Table 1 for the time windows specified, using all data that fall within 5-8 ‰ of these values, recognizing that a wider range (8 ‰) may be necessary to capture the higher variability during the transitional deglacial period in comparison to the modern and LGM, which display lower variability. Extending such screening criteria further back in time becomes more challenging given the increasing influence of diagenetic overprinting on the coral $\delta^{234}U_i$ values and merits further study.

5. Conclusions

This study presents a compilation of shallow and deep-sea coral U-series chemistry to evaluate the $\delta^{234}U$ value of modern seawater, and whether that value changed from the LGM to present. By normalizing uranium isotope ratios using the same decay constant and further normalizing data that was calibrated to a SE standard using SRM 960 measurements, we have determined that the modern $\delta^{234}U$ value of seawater is 145.0 ± 1.5 ‰, as recorded by corals and by direct measurements of seawater. Analysis of the shallow-water fossil coral record indicates that coral $\delta^{234}U_i$ and, by extension, mean surface ocean $\delta^{234}U$ was 5-7 ‰ lower than present during the LGM and that this difference is statistically significant. We have demonstrated that this shift cannot be explained as an artifact of poor preservation, or by invoking temporal biasing due to other factors such as location or coral taxa. Therefore, we conclude that the deglacial shift reflects a change in the primary geochemistry of the corals, which in turn records variability in $\delta^{234}U_{sw}$.

The deep-sea coral compilation also displays a deglacial positive shift in $\delta^{234}U$. Increased scatter and gaps in the data make this dataset more challenging to interpret unambiguously, however some interesting observations can still be made. The data display some differences in the magnitude of the changes between ocean basins, as well as differences in intra-basin variability within a given time slice. However, we note that higher $\delta^{234}U$ values observed in the North Atlantic and Southern Ocean are consistent with the mechanistic scenario where high-latitude physical weathering of U-bearing minerals is driving the shift in seawater composition through time.

We conclude that the practice of using an invariant screening value equivalent to modern seawater $\delta^{234}U$ to identify altered, shallow-water fossil corals should be revised. As a general guideline, for radiocarbon data, the current IntCal protocol should be revised to reflect the adjusted values of 145 ± 8 ‰ for corals younger than 17 ka and 140 ± 8 ‰ corals between 17 and 60 ka. This screening can be further refined for the deglaciation and LGM using the weighted means for the time windows listed in Table 2.

To better constrain $\delta^{234}U_i$ variability in fossil corals and identify any influence from diagenetic overprinting, future work should focus on:

(1) understanding why there is ± 5 ‰ variability in the $^{234}U/^{238}U$ activity ratios of modern corals;

(2) additional site-specific measurements of coral $\delta^{234}U_i$ – ideally measured within the same lab group – that cover the glacial-interglacial transition at the end of the LGM to evaluate the potential for shorter term variability;

(3) improving our understanding of diagenetic processes that modify the U and Th isotope compositions of fossil corals; and

(4) developing additional means of detecting primary versus diagenetic signals in older (>60 ka) fossil corals to assess open-system behavior.

Additionally, the analysis presented here highlights the need to increase the standardization and transparency of data-reporting practices within the U-series community as outlined in (Dutton et al., 2017). Using this approach will improve the longevity of the data as well as increasing the resolution to which we can resolve potential inter-basin offsets in $\delta^{234}U$ and determining whether millennial-scale phenomena (e.g. Heinrich events; Esat and Yokoyama, 2010) can have a discernable impact on the U-isotopic composition of seawater.

Acknowledgements

Support for this research was provided by NSF-DIBBS #1443037 (subaward to A.D.) and NSF-OCE award #1702740 to A.D. We thank D. Richards, M. Andersen and an anonymous reviewer for their constructive comments that improved the manuscript. We would also like to acknowledge our colleagues in the U-series discipline and members of the PALSEA2 working group funded by PAGES and INQUA for valuable discussions over the past several years.

Appendix A. Supplementary Information

Supplementary data associated with this article can be found in the online version.

References

Amiotte Suchet P., Probst J. L. and Ludwig W. (2003) Worldwide distribution of continental rock lithology: Implications for the atmospheric/soil CO_2 uptake by continental weathering and alkalinity river transport to the oceans. *Global Biogeochem. Cycles* **17**.

Andersen M. B., Elliott T., Freymuth H., Sims K. W. W., Niu Y. and Kelley K. A. (2015) The terrestrial uranium isotope cycle. *Nature* **517**, 356–359.

Andersen M. B., Erel Y. and Bourdon B. (2009) Experimental evidence for ^{234}U-^{238}U fractionation during granite weathering with implications for $^{234}U/^{238}U$ in natural waters. *Geochim. Cosmochim. Acta* **73**, 4124–4141.

Andersen M. B., Romaniello S., Vance D., Little S. H., Herdman R. and Lyons T. W. (2014) A modern framework for the interpretation of $^{238}U/^{235}U$ in studies of ancient ocean redox. *Earth Planet. Sci. Lett.* **400**, 184–194..

Andersen M. B., Stirling C. H., Potter E. K. and Halliday A. N. (2004) Toward epsilon levels of measurement precision on $^{234}U/^{238}U$ by using MC-ICPMS. *Int. J. Mass Spectrom.* **237**, 107–118.

Andersen M. B., Stirling C. H. and Weyer S. (2017) Uranium Isotope Fractionation. Rev. Mineral. Geochemistry 82.1, 799–850.

Andersen M. B., Stirling C. H., Zimmermann B. and Halliday A. N. (2010) Precise determination of the open ocean $^{234}U/^{238}U$ composition. *Geochemistry, Geophys. Geosystems* **11**.

Andersen M. B., Vance D., Keech A. R., Rickli J. and Hudson G. (2013) Estimating U fluxes in a high-latitude, boreal post-glacial setting using U-series isotopes in soils and rivers. *Chem. Geol.* **354**, 22–32.

Bard E., Fairbanks R. G., Hamelin B., Zindler A. and Chi Track Hoang (1991) Uranium-234 anomalies in corals older than 150,000 years. *Geochim. Cosmochim. Acta* **55**, 2385–2390.

Basu A., Brown S. T., Christensen J. N., Depaolo D. J., Reimus P. W., Heikoop J. M., Woldegabriel G., Simmons A. M., House B. M., Hartmann M. and Maher K. (2015) Isotopic and geochemical tracers for U(VI) reduction and U mobility at an in situ recovery U mine. Environ. Sci. Technol. 49, 5939–5947.

de Bievre, P., Lauer, K. F., and le Duigou, Y. (1971) Half-Life of ^{234}U. *Central Bureau for Nuclear Measurements*, Geel, Belgium.

Chabaux F., Ma L., Stille P., Pelt E., Granet M., Lemarchand D., Roupert R. di C. and Brantley S. L. (2011) Determination of chemical weathering rates from U series nuclides in soils and weathering profiles: Principles, applications and limitations. *Appl. Geochemistry* **26**, 20–23.

Chabaux F., Riotte J., & Dequincey O. (2003) U-Th-Ra fractionation during weathering and river transport. *Rev. in Mineral. Geochemistry* ***52*****(1)**, 533-576.

Charette M. A., Moore W. S. and Burnett W. C. (2008) Uranium-and Thorium-Series Nuclides as Tracers of Submarine Groundwater Discharge. *Radioact. Environ. Environ.* **13**, 234–289.

Chen J. H., Lawrence Edwards R. and Wasserburg G. J. (1986) ^{238}U, ^{234}U and ^{232}Th in seawater. *Earth Planet. Sci. Lett.* **80**, 241–251.

Chen T., Chen T., Robinson L. F., Beasley M. P., Claxton L. M., Andersen M. B., Lauren J., Wadham J., Fornari D. J. and Harpp K. S. (2016) Ocean mixing and ice-sheet control of seawater ^{234}U/^{238}U during the last deglaciation. *Science* **1015**, 626–629.

Cheng H., Adkins J., Edwards R. L. and Boyle E. A. (2000) U-Th dating of deep-sea corals. *Geochim. Cosmochim. Acta* **64**, 2401–2416.

Cheng H., Edwards R. L., Hoff J., Gallup C. D., Richards D. A. and Asmerom Y. (2000) The half-lives of uranium-234 and thorium-230. *Chem. Geol.* **169**, 17–33.

Cheng H., Lawrence Edwards R., Shen C. C., Polyak V. J., Asmerom Y., Woodhead J., Hellstrom J., Wang Y., Kong X., Spötl C., Wang X. and Calvin Alexander E. (2013) Improvements in ^{230}Th dating, ^{230}Th and ^{234}U half-life values, and U-Th isotopic measurements by multi-collector inductively coupled plasma mass spectrometry. *Earth Planet. Sci. Lett.* **371**–**372**, 82–91.

Chiu T. C., Fairbanks R. G., Mortlock R. A. and Bloom A. L. (2005) Extending the radiocarbon calibration beyond 26,000 years before present using fossil corals. *Quat. Sci. Rev.* **24**, 1797–1808.

Clark P., Dyke A., Shakun J., Carlson A., Clark J., Wohlfarth B., Mitrovica J., Hostetler S. and McCabe M. (2009) The Last Glacial Maximum. *Science* **325**, 710–714. Available at: citeulike-article-id:5391015%5Cnhttp://dx.doi.org/10.1126/science.1172873.

Cobb K. M., Charles C. D., Cheng H., Kastner M. and Edwards R. L. (2003) U/Th-dating living and young fossil corals from the central tropical Pacific. *Earth Planet. Sci. Lett.* **210**, 91–103.

Cowan G. A. and Adler H. H. (1976) The variability of the natural abundance of ^{235}U. *Geochim. Cosmochim. Acta* **40**, 1487–1490.

Crocket K. C., Vance D., Foster G. L., Richards D. A. and Tranter M. (2012) Continental weathering fluxes during the last glacial/interglacial cycle: Insights from the marine sedimentary Pb isotope record at Orphan Knoll, NW Atlantic. *Quat. Sci. Rev.* **38**, 89–99.

Delanghe D., Bard E. and Hamelin B. (2002) New TIMS constraints on the uranium-238 and uranium-234 in seawaters from the main ocean basins and the Mediterranean Sea. *Mar. Chem.* **80**, 79–93.

DePaolo D. J., Lee V. E., Christensen J. N. and Maher K. (2012) Uranium comminution ages: Sediment transport and deposition time scales. *Comptes Rendus - Geosci.* **344**, 678–687.

Deschamps P., Durand N., Bard E., Hamelin B., Camoin G., Thomas A. L., Henderson G. M., Okuno J. and Yokoyama Y. (2012) Ice-sheet collapse and sea-level rise at the Bølling warming 14,600 years ago. *Nature* **483**, 559–564.

Dosseto A. and Schaller M. (2016) The erosion response to Quaternary climate change quantified using uranium isotopes and in situ-produced cosmogenic nuclides. *Earth-Science Rev.* **155**, 60–81.

Dunk R. M., Mills R. A. and Jenkins W. J. (2002) A reevaluation of the oceanic uranium budget for the Holocene. *Chem. Geol.* **190**, 45–67.

Dürr H. H., Meybeck M. and Dürr S. H. (2005) Lithologic composition of the Earth's continental surfaces derived from a new digital map emphasizing riverine material transfer. *Global Biogeochem. Cycles* **19**, 1–23.

Dutton A., Rubin K., Mclean N., Bowring J., Bard E., Edwards R. L., Henderson G. M., Reid M. R., Richards D. A., Sims K. W. W., Walker J. D. and Yokoyama Y. (2017) Quaternary Geochronology Data reporting standards for publication of U-series data for geochronology and timescale assessment in the earth sciences. *Quat. Geochronol.* **39**, 142–149.

Edwards R. L., Chen J. H., Ku T. L. and Wasserburg G. J. (1987) Precise timing of the last interglacial period from mass spectrometric determination of thorium-230 in corals. *Science* **236**, 1547–1553.

Edwards R. L., Gallup C. D. and Cheng H. (2003) Uranium-series Dating of Marine and Lacustrine Carbonates. *Rev. Mineral. Geochemistry* **52**, 363–405.

Esat T. M. and Yokoyama Y. (2010) Coupled uranium isotope and sea-level variations in the oceans. *Geochim. Cosmochim. Acta* **74**, 7008–7020.

Esat T. M. and Yokoyama Y. (2006) Variability in the uranium isotopic composition of the oceans over glacial-interglacial timescales. *Geochim. Cosmochim. Acta* **70**, 4140–4150.

Fairbanks R. G., Mortlock R. A., Chiu T. C., Cao L., Kaplan A., Guilderson T. P., Fairbanks T. W., Bloom A. L., Grootes P. M. and Nadeau M. J. (2005) Radiocarbon calibration curve spanning 0 to 50,000 years BP based on paired $^{230}Th/^{234}U/^{238}U$ and ^{14}C dates on pristine corals. *Quat. Sci. Rev.* **24**, 1781–1796.

Foster G. L. and Vance D. (2006) Negligible glacial-interglacial variation in continental chemical weathering rates. *Nature* **444**, 918–921.

Fruijtier C., Elliott T. and Schlager W. (2000) Mass-spectrometric ^{234}U-^{230}Th ages from the Key Largo Formation, Florida Keys, United States: constraints on diagenetic age disturbance. *GSA Bulletin* **112(2)**, 267-277.

Galewsky J., Silver E. A., Gallup C. D., Edwards R. L. and Potts D. C. (1996) Foredeep tectonics and carbonate platform dynamics in the Huon Gulf, Papua New Guinea. *Geology* **24**, 819–822.

Gallup C. D., Edwards R. L. and Johnson R. G. (1994) The timing of high sea levels over the

past 200,000 years. *Science* **263**, 796–800.

Gutjahr M., Frank M., Halliday A. N. and Keigwin L. D. (2009) Retreat of the Laurentide ice sheet tracked by the isotopic composition of Pb in western North Atlantic seawater during termination 1. *Earth Planet. Sci. Lett.* **286**, 546–555.

Hamelin B., Bard E., Zindler A. and Fairbanks R. G. (1991) $^{234}U/^{238}U$ mass spectrometry of corals: How accurate is the UTh age of the last interglacial period? *Earth Planet. Sci. Lett.* **106**, 169–180.

Hartmann J. and Moosdorf N. (2012) The new global lithological map database GLiM: A representation of rock properties at the Earth surface. *Geochemistry, Geophys. Geosystems* **13**, 1–37.

Hemming S. R. (2004) Heinrich events: Massive late Pleistocene ditritus layers of the North Atlanitc and their global cliamate imprint. *Rev. Geophys.* **42**.

Henderson G. M. (2002) Seawater ($^{234}U/^{238}U$) during the last 800 thousand years. *Earth Planet. Sci. Lett.* **199**, 97–110.

Henderson G. M. and Anderson R. F. (2003) The U-series toolbox for paleoceanography. *Rev. Mineral. Geochemistry* **52**, 493–531.

Henderson G. M., Hall B. L., Smith A. and Robinson L. F. (2006) Control on ($^{234}U/^{238}U$) in lake water: A study in the Dry Valleys of Antarctica. *Chem. Geol.* **226**, 298–308.

Hibbert F. D., Rohling E. J., Dutton A., Williams F. H., Chutcharavan P. M., Zhao C. and Tamisiea M. E. (2016) Coral indicators of past sea-level change: A global repository of U-series dated benchmarks. *Quat. Sci. Rev.* **145**, 1–56.

Jaffey A. H., Flynn K. F., Glendenin L. E., Bentley W. C. and Essling A. M. (1971) Precision measurement of half-lives and specific activities of U^{235} and U^{238}. *Phys. Rev. C* **4**, 1889–1906.

Kurzweil F., Gutjahr M., Vance D. and Keigwin L. (2010) Authigenic Pb isotopes from the Laurentian Fan: Changes in chemical weathering and patterns of North American freshwater runoff during the last deglaciation. *Earth Planet. Sci. Lett.* **299**, 458–465.

Lambeck K., Rouby H., Purcell A., Sun Y. and Sambridge M. (2014) Sea level and global ice volumes from the Last Glacial Maximum to the Holocene. *Proc. Natl. Acad. Sci.* **111**, 15296–15303.

Lounsbury M., and Durham R. W. (1971) Alpha half-life of ^{234}U. *Atomic Energy of Canada Ltd.*, Chalk River, Ont.

Ma L., Chabaux F., Pelt E., Blaes E., Jin L. and Brantley S. (2010) Regolith production rates calculated with uranium-series isotopes at Susquehanna/Shale Hills Critical Zone Observatory. *Earth Planet. Sci. Lett.* **297**, 211–225.

Meadows J., Armani R., Callis E. and Essling A. (1980) Half-life of ^{230}Th. *Phys. Rev. C* **22**, 750–

754.

Murphy M. J., Stirling C. H., Kaltenbach A., Turner S. P. and Schaefer B. F. (2014) Fractionation of $^{238}U/^{235}U$ by reduction during low temperature uranium mineralisation processes. Earth Planet. Sci. Lett. 388, 306–317.

Noordmann J., Weyer S., Georg R. B., Jöns S. and Sharma M. (2016) $^{238}U/^{235}U$ isotope ratios of crustal material, rivers and products of hydrothermal alteration: new insights on the oceanic U isotope mass balance. *Isotopes Environ. Health Stud.* **52**, 141–163.

Palmer M. R., and Edmond J. M. (1993) Uranium in river water. *Geochim. Cosmochim. Acta* **57(20)**, 4947-4955.

Reimer P. J., Bard E., Bayliss A., Beck J. W., Blackwell P. G., Ramsey C. B., Brown D. M., Buck C. E., Edwards R. L., Friedrich M., Grootes P. M., Guilderson T. P., Haflidason H., Hajdas I., Hatte C., Heaton T. J., Hogg A. G., Hughen K. A., Kaiser K. F., Kromer B., Manning S. W., Reimer R. W., Richards D. A., Scott E. M., Southon J. R., Turney C. S. M., and van der Plicht J. (2013) Selection and Treatment of Data for Radiocarbon Calibration: An Update to the International Calibration (IntCal) Criteria. *Radiocarbon* **55**, 1923–1945.

Reyes A. V, Carlson A. E., Beard B. L., Hatfield R. G., Stoner J. S., Winsor K., Welke B. and Ullman D. J. (2014) South Greenland ice-sheet collapse during Marine Isotope Stage 11. *Nature* **510**, 525–8.

Robinson L. F., Adkins J. F., Fernandez D. P., Burnett D. S., Wang S. L., Gagnon A. C. and Krakauer N. (2006) Primary U distribution in scleractinian corals and its implications for U series dating. *Geochemistry, Geophys. Geosystems* **7**.

Robinson L. F., Belshaw N. S. and Henderson G. M. (2004) U and Th concentrations and isotope ratios in modern carbonates and waters from the Bahamas. *Geochim. Cosmochim. Acta* **68**, 1777–1789.

Robinson L. F., Henderson G. M., Hall L. and Matthews I. (2004) Climatic control of riverine and seawater uranium-isotope ratios. *Science* **305**, 851–854.

Scholz D. and Mangini A. (2007) How precise are U-series coral ages? *Geochim. Cosmochim. Acta* **71**, 1935–1948.

Scholz D., Mangini A. and Meischner D. (2007) 9. U-redistribution in fossil reef corals from Barbados, West Indies, and sea-level reconstruction for MIS 6.5. *Dev. Quat. Sci.* **7**, 119–139.

Shen C. C., Li K. S., Sieh K., Natawidjaja D., Cheng H., Wang X., Edwards R. L., Lam D. D., Hsieh Y. Te, Fan T. Y., Meltzner A. J., Taylor F. W., Quinn T. M., Chiang H. W. and Kilbourne K. H. (2008) Variation of initial $^{230}Th/^{232}Th$ and limits of high precision U-Th dating of shallow-water corals. *Geochim. Cosmochim. Acta* **72**, 4201–4223.

Steiger R. H. and Jäger E. (1977) Subcommission on geochronology: Convention on the use of decay constants in geo- and cosmochronology. *Earth Planet. Sci. Lett.* **36**, 359–362.

Stirling C. H. and Andersen M. B. (2009) Uranium-series dating of fossil coral reefs: Extending the sea-level record beyond the last glacial cycle. *Earth Planet. Sci. Lett.* **284**, 269–283.

Stirling C. H., Andersen M. B., Potter E. K. and Halliday A. N. (2007) Low-temperature isotopic fractionation of uranium. *Earth Planet. Sci. Lett.* **264**, 208–225.

Stirling C. H., Esat T. M., McCulloch M. T. and Lambeck K. (1995) High-precision U-series dating of corals from Western Australia and implications for the timing and duration of the Last Interglacial. *Earth Planet. Sci. Lett.* **135**, 115–130.

Thomas A. L., Henderson G. M., Deschamps P., Yokoyama Y., Mason A. J., Bard E., Hamelin B., Durand N. and Camoin G. (2009) Penultimate deglacial sea-level timing from uranium/thorium dating of Tahitian corals. *Science* **324**, 1186–1189.

Thompson W. G., Spiegelman M. W., Goldstein S. L. and Speed R. C. (2003) An open-system model for U-series age determinations of fossil corals. *Earth Planet. Sci. Lett.* **210**, 365–381.

Tissot F. L. H. and Dauphas N. (2015) Uranium isotopic compositions of the crust and ocean: Age corrections, U budget and global extent of modern anoxia. Geochim. Cosmochim. Acta 167, 113–143.

Walker M., Johnsen S., Rasmussen S. O., Popp T., Steffensen J. P., Gibbard P., Hoek W., Lowe J., Andrews J., Bjorck S., Cwynar L. C., Hughen K., Kershaw P., Kromer B., Litt T., Lowe D. J., Nakagawa T., Newnham R. and Schwander J. (2009) Formal definition and dating of the GSSP (Global Stratotype Section and Point) for the base of the Holocene using the Greenland NGRIP ice core, and selected auxiliary records. *J. Quat. Sci.* **24**, 3–17.

Weyer S., Anbar A. D., Gerdes A., Gordon G. W., Algeo T. J. and Boyle E. A. (2008) Natural fractionation of $^{238}U/^{235}U$. *Geochim. Cosmochim. Acta* **72**, 345–359.

Wilson D. J., van de Flierdt T. and Adkins J. F. (2017) Lead isotopes in deep-sea coral skeletons : Ground-truthing and a first deglacial Southern Ocean record. *Geochim. Cosmochim. Acta* **204**, 350–374.

Yokoyama Y., Esat T. M. and Lambeck K. (2001) Last glacial sea-level change deduced from uplifted coral terraces of Huon Peninsula, Papua New Guinea. *Quat. Int.* **83–85**, 275–283.

Yu K., Zhao J., Roff G., Lybolt M., Feng Y., Clark T. and Li S. (2012) High-precision U-series ages of transported coral blocks on Heron Reef (southern Great Barrier Reef) and storm activity during the past century. *Palaeogeogr. Palaeoclimatol. Palaeoecol.* **337–338**, 23–36.

Zhou J., Lundstrom C. C., Fouke B., Panno S., Hackley K. and Curry B. (2005) Geochemistry of speleothem records from southern Illinois: Development of $(^{234}U)/(^{238}U)$ as a proxy for paleoprecipitation. *Chem. Geol.* **221**, 1–20.

Tables

Table 1
Means and statistical tests for screened corals

Age Range	n	IVWM[a]		Median		t-test (two-sided)			Bootstrap
		$\delta^{234}U_i$ (‰)	2σ (‰)	$\delta^{234}U_i$ (‰)	1 sd[b] (‰)	p-value	t-value	df[c]	p-value
Modern (0-0.3 ka)	137	145.0	1.5	145.1	1.8	N/A	N/A	N/A	N/A
Interglacial (0.3-11.7 ka)	436	144.8	0.9	144.5	4.6	0.02	-2.4	435	0
Deglacial (11.7-17 ka)	300	143.7	0.8	143.6	3.9	<<0.01	-7.7	299	0
Early Deglacial (17-21 ka)	59	140.7	1.1	141	2.3	<<0.01	-14.1	58	0
LGM (21-29 ka)	41	137.8	1.1	137.8	2.3	<<0.01	-19.8	40	0

[a]IVWM = Inverse variance weighted mean

[b]Standard deviation

[c]Degrees of freedom

Table 2
Decay constant values referenced in this study. Units are decays per year (dpy).

Identifier	$\lambda^{238}U$ (dpy)	$\lambda^{234}U$ (dpy)	$\lambda^{230}Th$ (dpy)	Source(s)
D1	1.55125E-10	2.835E-06	9.195E-06	Lounsbury and Durham (1971); de Bievre et al. (1971); Jaffey et al. (1971); Meadows et al. (1980)
D2	1.55125E-10	2.8262E-06	9.158E-06	Jaffey et al. (1971); Cheng et al. (2000)
D3	1.55125E-10	2.82206E-06	9.1705E-06	Jaffey et al. (1971); Cheng et al. (2013)

Table 3
Sources for coral and seawater $\delta^{234}U$ measurements from figure 1.

Study #	n	Reference	U-standard calibration
1	24	Delanghe et al. (2002)	Gravimetric
2	14	Robinson et al. (2004)	Gravimetric
3	25	Shen et al. (2008)	Gravimetric
4	19	Andersen et al. (2010)	Secular Equilibrium
5	2	Edwards et al. (1987)	Gravimetric
6	3	Stirling et al. (1995)	Secular Equilibrium
7	22	Galewsky et al. (1996)	Gravimetric
8	6	Delanghe et al. (2002)	Gravimetric
9	29	Cobb et al. (2003)	Gravimetric
10	7	Robinson et al. (2004, coral)	Gravimetric
11	4	Robinson et al. (2004, other carbonates)	Gravimetric
12	56	Shen et al. (2008)	Gravimetric
13	108	Yu et al. (2012)	Gravimetric
14	137	This Study (Modern)	N/A
14	41	This Study (LGM 29-21 ka)	N/A

Table 4
Inverse variance weighted means for Pacific and Atlantic shallow water corals

Age Range	IVWM (Atlantic)[a]			IVWM (Pacific)[a]		
	n	$\delta^{234}U_i$ (‰)	2σ	n	$\delta^{234}U_i$ (‰)	2σ
Modern (0-0.3 ka)	12	144.4	1.8	125	145	1.4
Interglacial (0.3-8 ka)	82	144.8	0.5	352	144.7	1.3
Deglacial (8-17 ka)	92	143.9	0.8	208	143.6	0.8
Early Deglacial (17-21 ka)	43	140.6	1.0	16	140.9	1.2
LGM (21-29 ka)	26	137.1	1.0	15	139.8	1.4

[a]IVWM = Inverse variance weighted mean

Figure Captions

Fig. 1. Modern $\delta^{234}U$ measurements of modern seawater and corals. (a) Published $\delta^{234}U$ values, in permil, for modern seawater (yellow squares) and modern corals (blue circles), and calculated for the entire data compilation for modern and LGM corals (red diamonds). Data sources are provided in Table 3. D1, D2, and D3 refer to different decay constant values for ^{234}U and ^{230}Th (Table 2). The solid and dashed gray lines are the weighted mean value and 2σ uncertainty, respectively, for modern corals compiled in this study. (b) Same data as (a), but normalized to D3. Black arrows denote samples that were calibrated to a secular equilibrium standard (Section 2.1) and show the shift induced by normalizing to SRM 960 measurements. Transparent data points are the reported values prior to applying the SRM 960 correction. In the case of source 6 (Stirling et al., 1995) we have used the more recent SRM 960 values reported by McCulloch and Mortimer (2008) and have removed the -2.1 ‰ $\delta^{234}U$ correction assigned by Stirling et al. (1995). We have not plotted early measurements of $\delta^{234}U_{sw}$ (Chen et al., 1986) as we suspect that the ^{238}U tailing correction may have been overestimated using a linear extrapolation as hypothesized by Delanghe et al. (2002). For the orange square from source 4, the error bars are smaller than the data point.

Fig. 2. $\delta^{234}U_i$ variability in fossil corals over the past 60,000 years. (a) Shallow-water fossil coral $\delta^{234}U_i$ (blue circles) with 2σ uncertainties. The solid and dotted gray lines are the inverse-variance weighted mean value and 2σ uncertainty envelope, respectively, for modern corals compiled in this study; gray vertical bar denotes the timing of the Last Glacial Maximum as shown in (Clark et al., 2009). (b) A global mean sea level (GMSL) curve (Lambeck et al., 2014). (c) $^{206}Pb/^{204}Pb$ isotope ratios of ferromanganese deposits from Orphan Knoll in the North

Atlantic (Crocket et al., 2012). Dashed red lines indicate Heinrich events. (d) Boxplots (median and 1.5 times the interquartile range) of shallow-water corals for 5 time slices. 11 measurements in (a) and 4 measurements in (d) fall outside the plotted range.

Fig. 3. Shallow-water coral $\delta^{234}U_i$ plotted by ocean basin. The solid gray line represents the $\delta^{234}U_i$ value of modern seawater.

Fig. 4. Screened deep-sea coral $\delta^{234}U_i$ measurements compiled for this study. (a) Deep sea- coral data are plotted with screened shallow-water corals. (b) Deep-sea corals by latitudinal sector of the Atlantic Ocean. (c) Deep-sea corals by ocean basin for the Southern Ocean, Pacific Ocean, and Mediterranean Sea. Gray bars represent the modern $\delta^{234}U$ value of seawater. Deep-sea corals with [^{232}Th] > 2 ppb have been screened out.

Fig. 5. Speleothem records of $\delta^{234}U_i$ variability over the past 30,000 years. (a) Speleothem $\delta^{234}U_i$ measurements compiled by Chen et al. (2016) plotted by geographic location as percent change from the mean $\delta^{234}U_i$ value for each speleothem. Black vertical bar marks the beginning of the Holocene (Walker et al., 2009) with the solid grey bar denotes the LGM (Clark et al., 2009). (b) Boxplots of $\delta^{234}U_i$ values for screened shallow-water corals (blue font) superimposed on (c), a global mean sea level curve (Lambeck et al., 2014). Nine measurements fall outside the plotted range for the boxplot.

Fig. 6. Box model results for changes in surface ocean $\delta^{234}U_{sw}$ in response to 2, 5, and 10 kyr pulsing experiments. (a) Model outputs for a pulse of increased $\delta^{234}U_{input}$. (b) Model outputs for a

pulse of increased $^{238}U_{input}$. (c) Model inputs for (a). (d) Model inputs for (b). Outputs from each pulsing experiment have been uniformly shifted up/down so that the pulse starts at a $\delta^{234}U_{sw}$ value of 138 ‰.

Figure 7. Shallow-water coral $\delta^{234}U_i$ separated by (a) diagenetic environment. (b) Coral species/taxa. The solid gray line in (a) and (b) represents the $\delta^{234}U$ value of modern seawater.

Figure 8. Shallow-water coral $\delta^{234}U_i$ separated by site. The solid gray line represents the $\delta^{234}U$ value of modern seawater.

Figure 1

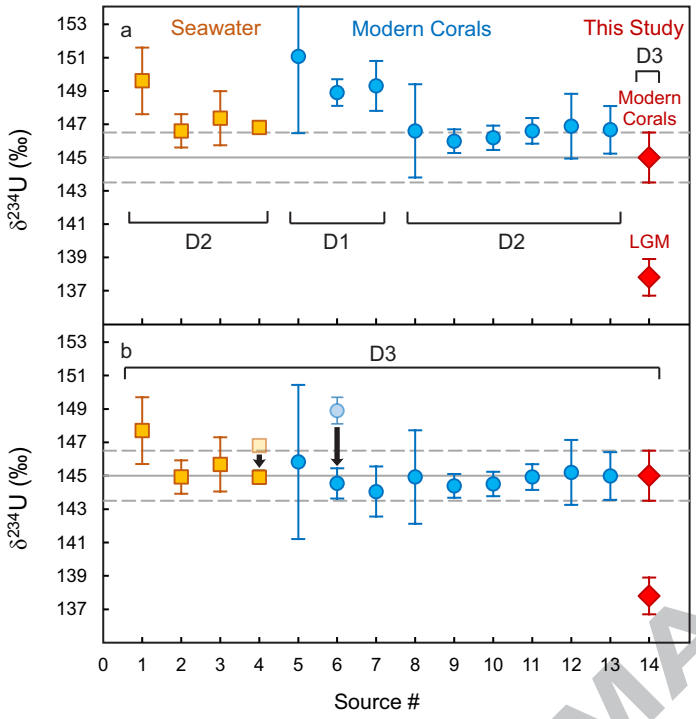

Figure 2

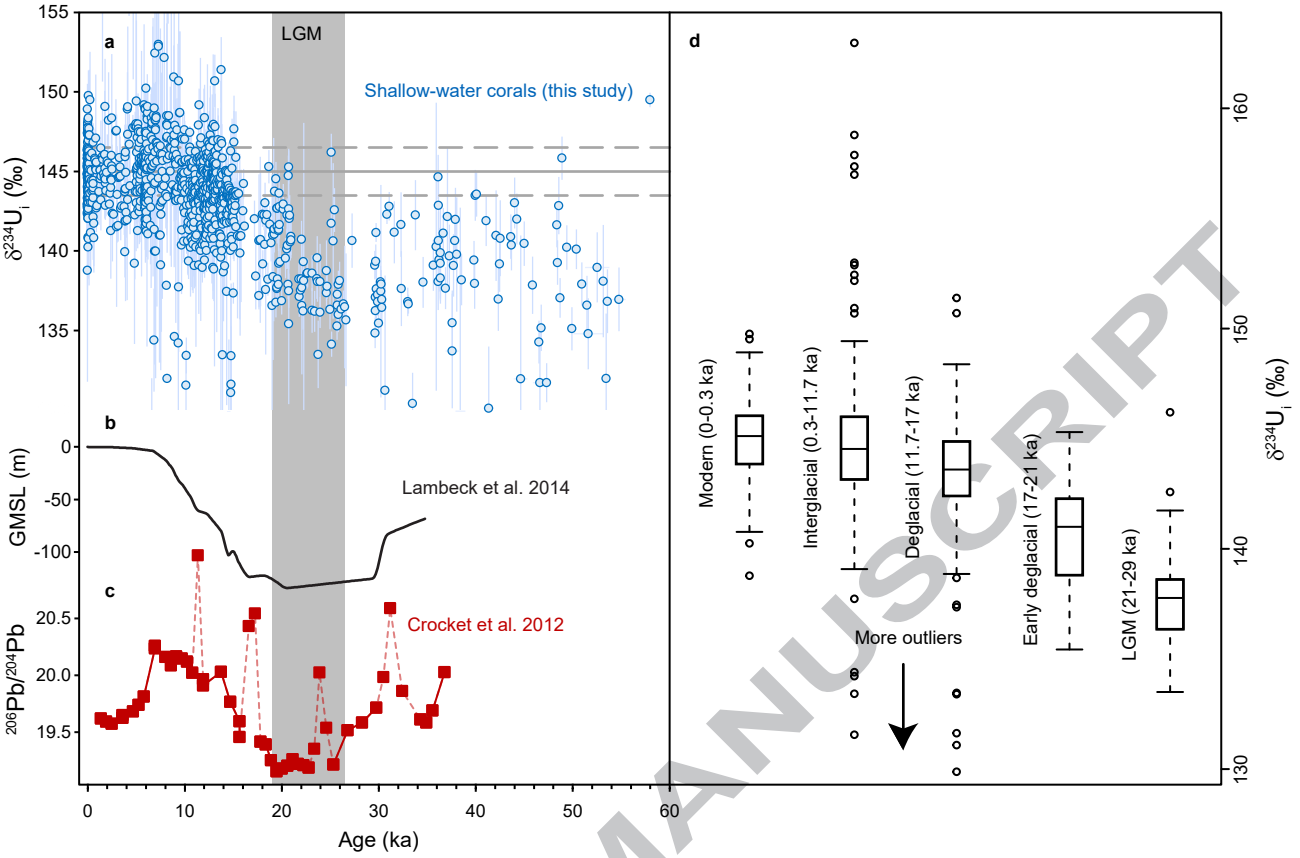

Figure 3

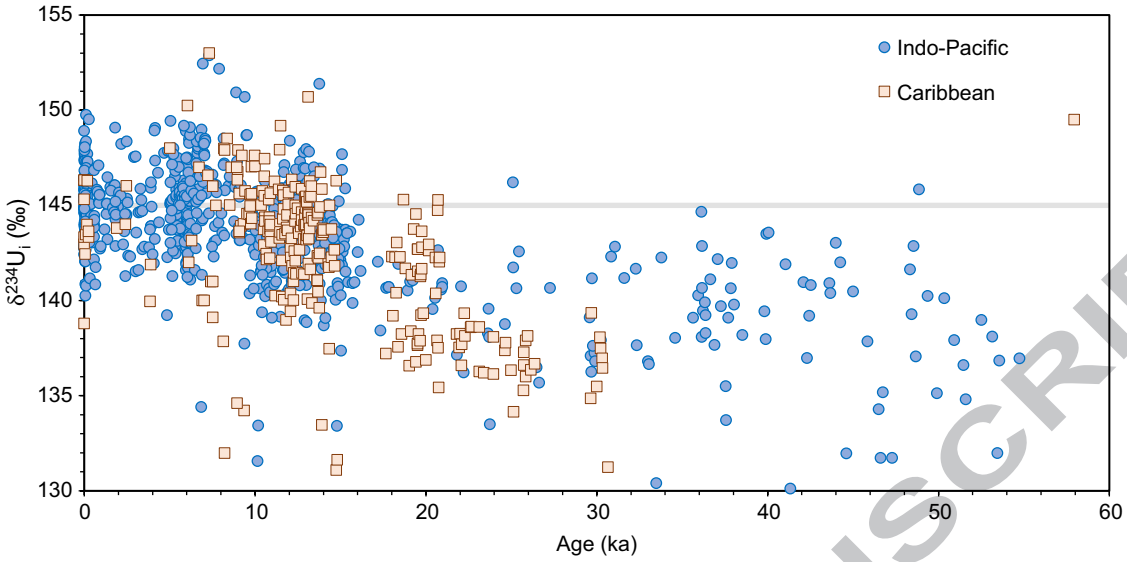

Figure 4

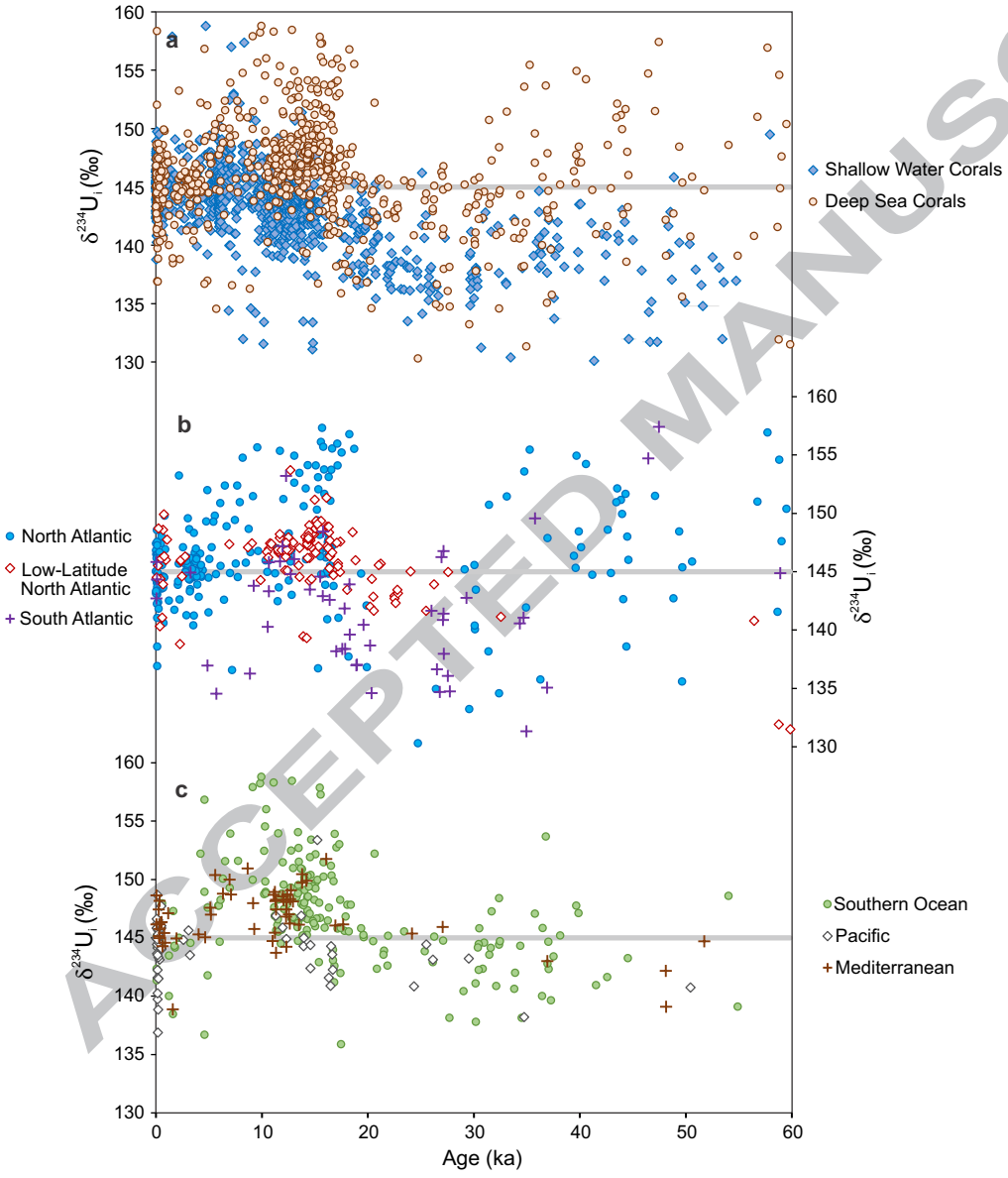

Figure 5

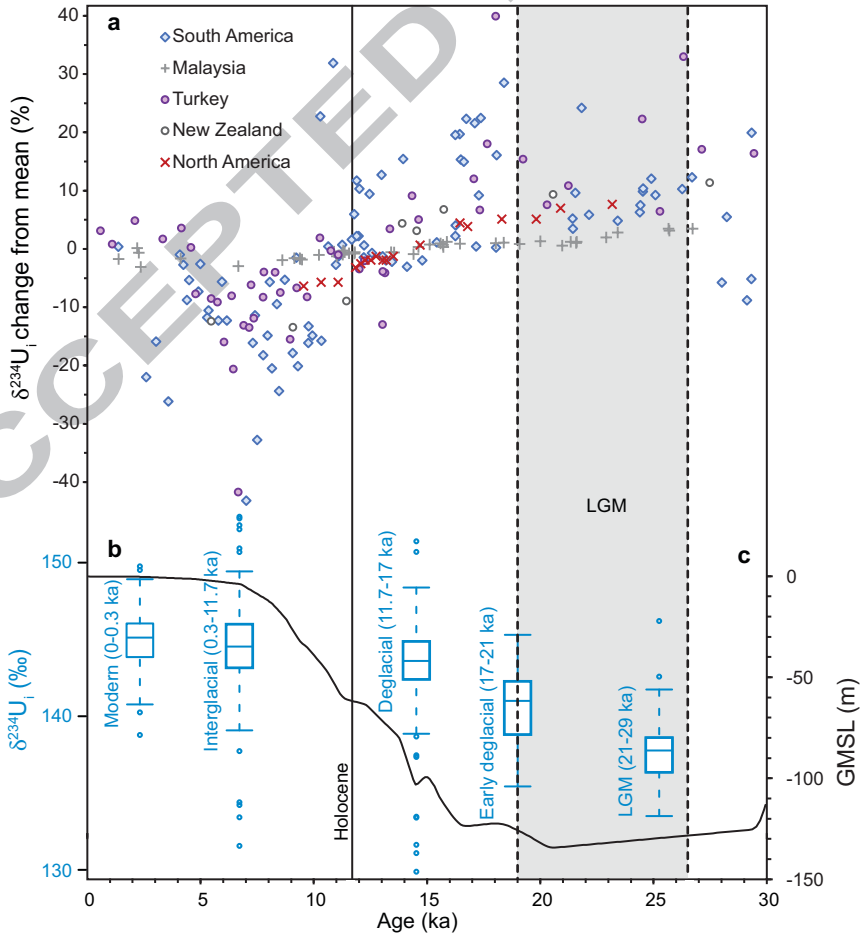

Figure 6

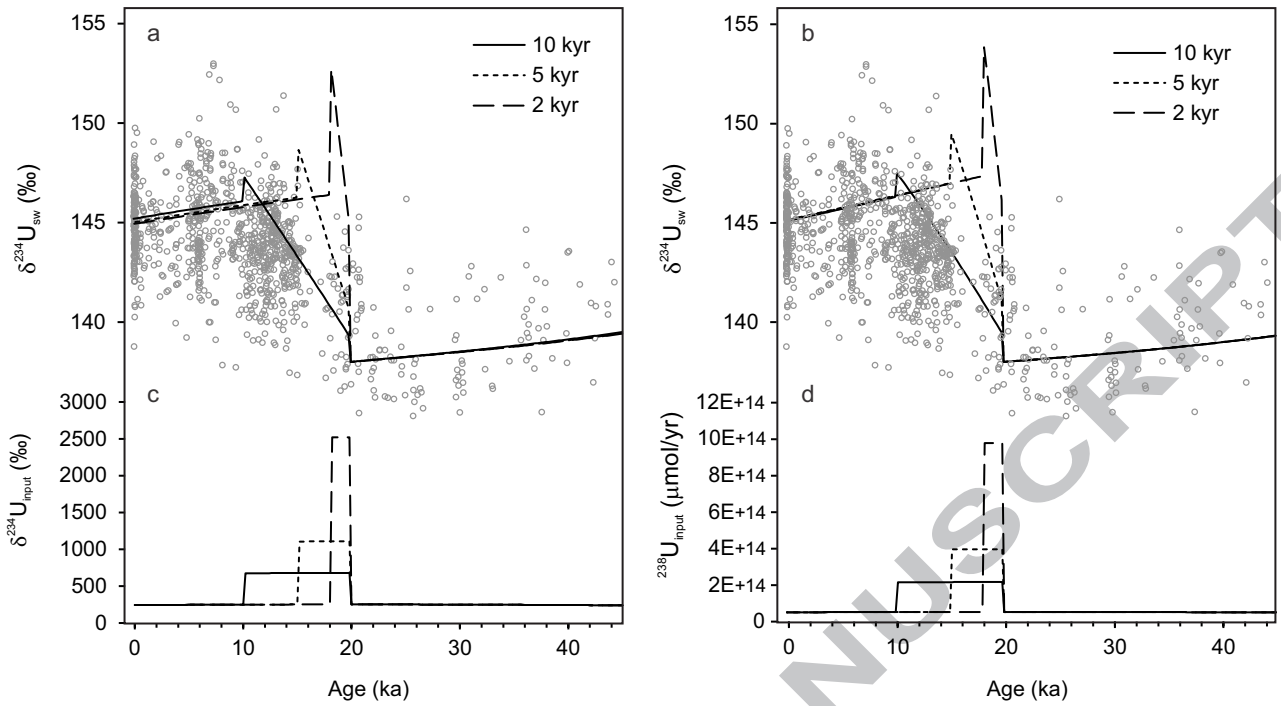

Figure 7

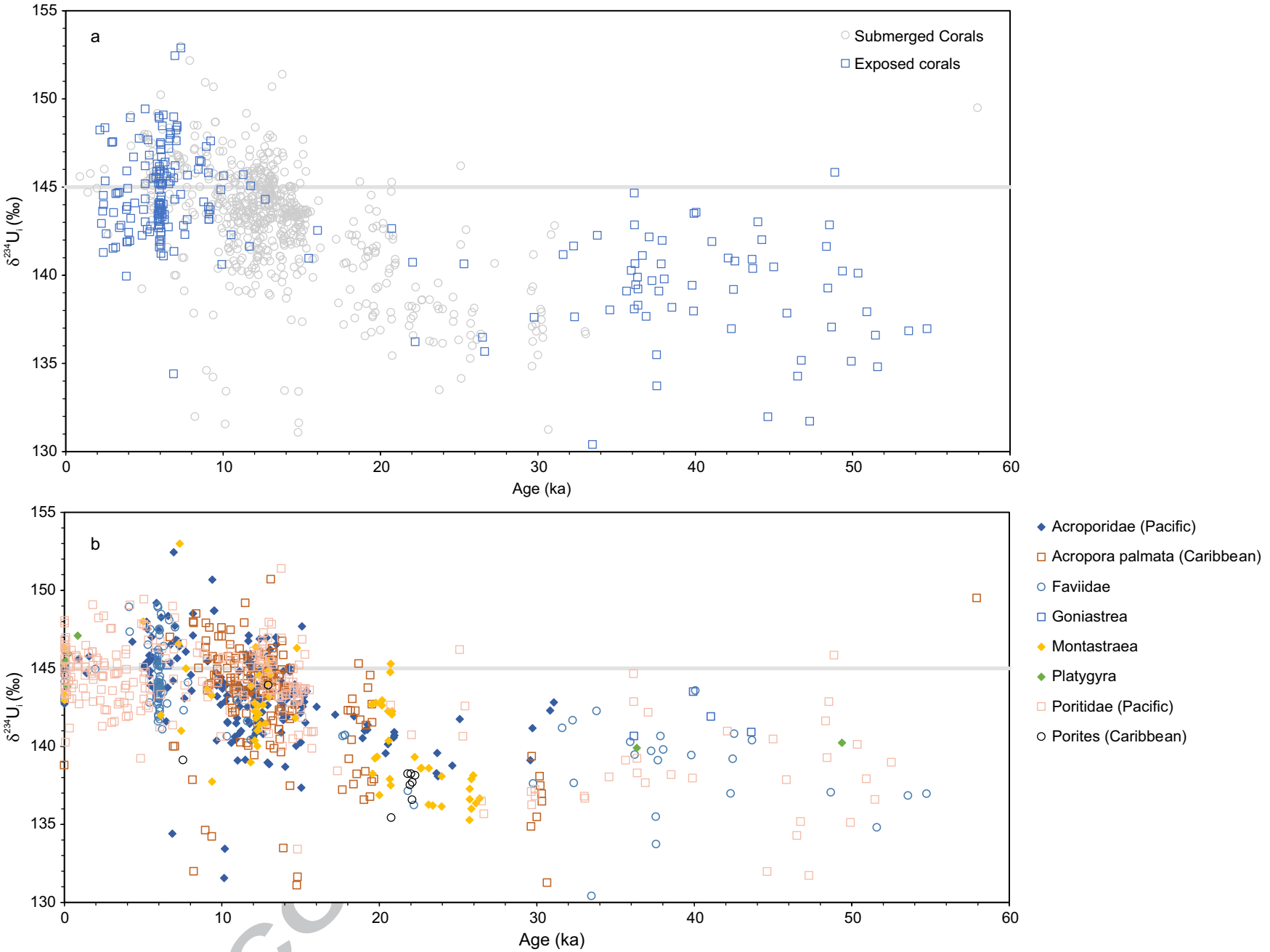

Figure 8